Paleoearthquake Magnitude Detection Limit Along the Himalayan Frontal Thrust

STEVEN G. WESNOUSKY

Center for Neotectonic Studies and Nevada Seismological Laboratory

University of Nevada, Reno

Reno, NV 89557

Email: wesnousky@unr.edu

Abstract

The largest historical earthquakes along the Himalayan Frontal Thrust reach values of Mw equal to MW 8.7-8.9. A considered view of historical and paleoseismological observations reveals no clear and substantive evidence that any has produced surface rupture along the Himalayan Frontal Thrust. The logical implication then is that the *paleoearthquake magnitude detection level* for earthquakes on the MHT is on the order of Mw >8.7: Large earthquakes with magnitudes less than this value may not be represented in the geologic record preserved in fault scarps along the Himalayan Frontal Thrust.

Introduction

It is generally accepted that the largest earthquakes along the Himalayan arc are the result of episodic release of stress that accumulates with the convergence of India into Tibet. The largest earthquakes are attributed to slip along the Main Himalayan Frontal Thrust (MHT), a north dipping shallow dipping decollement that intersects the surface to produce scarps that mark the trace of the Himalayan Frontal Thrust (HFT, **Figure 1**). Among the largest earthquakes attributed to slip on the decollement are the ~Mw 8.7-8.9 June 6 1505 (central Himalaya), the Mw 7.5-8.5 May 4, 1714 (Bhutan), the Mw 7.6-8 Sept 1 1803 (Almora), the Mw ~7.8 Aug 26, 1833 (Nepal), the Apr 4 1905 Mw 7.8 (Kangra), the Mw 8.4 Jan 15, 1934 (Bihar), the Mw 8.7 Aug 15, 1950 (Assam), and the most recent Mw 7.8 April 25, 2015 (Gorkha). The magnitudes and approximate source areas of the events are taken from Bilham's (2018)) recent synthesis of Himalaya earthquakes.

Continental earthquakes of Mw>7 outside of the Himalayan arc invariably produce surface rupture and fault scarps where the causative fault plane meets the surface of the earth (e.g. Wesnousky, 2008). The observation has for some time underpinned efforts to incorporate geology into assessing the size and recurrence time of large earthquakes on mapped faults for seismic hazard analysis (Wesnousky, 1986; Wesnousky et al., 1984), commonly with the application of paleoseismologic principles to exposures created by excavation of trenches across fault scarps (McCalpin, 1996, 2009). The approach is unable to provide insight to the recurrence time of earthquakes that are of insufficient dimension to rupture to the surface and displace youthful sediments. The value of paleoseismologic studies to assessing seismic hazard in a region is thus limited by the magnitude of earthquakes in a region that may be expected to produce surface rupture. Adopting the vernacular commonly used in seismic network studies, the value is here referred to as the *paleoearthquake magnitude detection threshold*. Observations relative to understanding that value along the Himalayan Frontal Thrust of Nepal and India are the topic of this paper.

Synopsis of Geological and Historical Observations Bearing on the Problem

The potential to assess the size of earthquakes that may be expected to produce surface rupture along the HFT resides in the historical record of earthquakes and the accumulating number of paleoseismologic studies along the HFT. Interpretations of historical and paleoseismological records come with distinctive sets of uncertainties. For example, temporal bounds on the age of scarps along the HFT arising from geological study are generally on the order of hundreds of years. Likewise, exact estimates of the size of earthquakes responsible for scarps along the HFT are coupled with large uncertainty bounds because along the Himalaya such estimates generally require assumption of fault dip that produces the vertical displacements recorded by the fault scarps, and furthermore the ultimate estimate of Mw rests on empirical correlations for historical earthquakes between either fault displacement or fault length which show large uncertainty bounds. Best estimates arising from geology are that HFT scarps are generally the result of earthquakes of at least Mw ~8.5 and likely greater. The source of these statements arises from Wesnousky (2020), a compilation and analysis of paleoseismic studies along the Himalayan Frontal Thrust.

The pre-instrumental record of earthquakes along the HFT including the time period prior to the early 20th century extends back to 1200 AD (Pant, 2002). Estimates of the Mw and dimension of rupture for these earthquakes are dependent on the spatial distribution of intensity observations along the arc. Most often inferences of Mw for earthquakes during the pre-instrumental era are limited to felt reports from a single locality and do not provide direct information whether or not they were accompanied by surface rupture along the HFT. The larger earthquakes along the Himalayan Frontal Thrust for which investigators have deemed isoseismal data sufficient to estimate the location, the approximate source area, and Mw of rupture are those few listed in the initial paragraph of this section occurring through the 16th to 20th centuries. Bilham (2018) provides analysis and citation of original studies that describe each event.

The lack of reported surface rupture along the HFT and confinement of higher intensity measurements to regions north of the HFT have been reason to suggest the source areas of the Mw 7.6-8 Sept 1 1803 Almora, Mw ~7.8 Aug 26 1833 Nepal, and Mw 7.8 April 4 1905 Kangra earthquakes occurred on the MHT but of insufficient size to rupture to the surface and produce scarps along the HFT. Isoseismal data allow argument that the central Himalaya earthquake of June 6 1505 was of Mw 8.7-8.9 and ruptured several hundred km or more of the MHT (Jackson, 2002). Historical accounts provide no descriptions of surface rupture along the HFT in 1505. Whether or not the absence is real or an artifact of limited historical accounts is uncertain. Scarps along the HFT in western India that post-date the late 1400s were posited by Kumar et al. (2006) to have possibly originated in the 1505 earthquake. They note that the scarps considered are not south of the main reports of damage in Nepal where they would be most expected if due to displacement on the underlying HFT but, rather, well to the west in India (**Figure 1**). So it remains at best uncertain whether or not this ~Mw 8.7-8.9 earthquake produced surface rupture along the HFT. The Mw 7.5-8.5 May 4, 1714 (Bhutan) earthquake has been speculated to have produced a scarp occurred after A.D. 1550 ± 100 and could correspond to the A.D. 1713 event: isoseismal data are sparse (**Figure 1**) and insufficient to assess the size of the event to better than a complete unit of magnitude (Ambraseys and Jackson, 2003; Berthet et al., 2014; Bilham, 2018; Hetenyi et al., 2016).

The size and spatial extent of earthquakes along the HFT that post-date the early twentieth century are better described with the advent of seismic instrumentation and more detailed historical accounts than earthquakes of earlier years. The largest include the Mw 8.4 Bihar earthquake of Jan 15, 1934, the Mw 8.7 Assam earthquake of Aug 15, 1950 (Assam), and the most recent Mw 7.8 Gorkha event of April 25, 2015. Geophysical and field studies show clearly that the Gorkha earthquake of 2015 was confined to deeper sections of the decollement and produced no surface rupture along the HFT (e.g., Angster et al., 2015; Hayes et al., 2015). Earthquakes of Mw 7.8 thus need not produce surface displacements along the HFT. The earthquake provides credence that earlier similar magnitude events of 1803 and 1833 were likewise confined on subsurface extents of the MHT. For the larger 1934 Mw 8.4 Bihar earthquake, historical accounts also include no reports of surface rupture along the HFT. Paleoseismic observations at one site within the 1934 isoseismal zone have been interpreted to indicate that the event produced surface rupture along the HFT (Bollinger et al., 2014; Sapkota et al., 2013), implying that historical accounts are simply insufficient to document surface rupture. Subsequent study shows that the principal observation on which the interpretation of 1934 surface rupture is based is incorrect and, as a result, there remains no definitive or substantive evidence of 1934 surface rupture (Wesnousky et al., 2018a). The great Mw 8.7 Assam earthquake of Aug 15, 1950 is the largest instrumentally recorded continental earthquake (USGS, 2021). Surface rupture is reasonably expected for an earthquake of this size. Two recent papers have attributed scarps along the HFT to the earthquake (Priyanka and Jayangondaperumal et al., 2017; Coudurier-Curveur et al., 2020). It is warranted to examine closely the observations reported in these two papers given their importance to the topic of this paper.

Examination of Interpretations of 1950 surface rupture.

The Priyanka et. al. (2017) paper states 'that the 15th August, 1050 Tibet-Assam earthquake (Mw~8.6) did break the eastern Himalayan front producing a coseismic slip of 5.5 ± 0.7 meters" in the municipality of Pasighat near the eastern limit of the Himalayan arc (**Figure 1**). The claim is based on interpretation of a trench exposure. The logs of the trench walls are reproduced in **Figure 2a**. It is interpreted that unit 2 was the ground surface and soil at the time of the 1950 earthquake. Logic yields that overlying units 3, 4, and 5 were deposited subsequent to displacements on the fault strands labeled F1 and F2. The radiocarbon ages shown for samples taken from both trench walls are grouped according to unit sampled and stratigraphic order in **Figure 2b**. Samples from both trench walls are included. The plot on the left is expanded on the right to more clearly show the youngest ages. There is a distinct bimodal distribution of ages with the majority of ages falling near the BC/AD boundary and the younger distribution that postdates ~1600 AD (**Figure SI3-2**). The units from which samples are taken are indicated by the last letters in the sample names listed.

Seven of the 9 samples in the U2 soil that is interpreted to have been active up until the 1950 earthquake show ages near the BC/AD boundary. The seven samples are derived from discrete pieces of charcoal. The final two samples from unit 2 are younger, with one (BS-1) showing a modern age and the other (BS-3) yielding an age of 1640-1950 AD. The authors interpret that the older samples reflect nearly 2000 years of residence time of the charcoal during transport, discard them in the analysis, and assert that the younger two samples record the age of the U2 deposit. The younger two sample ages are distinguished from the older samples by fact that they are derived from bulk soil samples rather than discrete charcoal samples. More often, ages derived from single charcoal samples are valued over bulk samples in assessing the age of a deposit. The layer from which bulk samples BS-1 and BS-3 are drawn is impregnated with modern roots **(Figure 3**) and there is a distinct possibility the bulk samples are contaminated by modern roots and their decay, an issue not addressed in the manuscript. The possible contamination is consistent with the observation that discrete detrital charcoal samples adjacent to each yield ages near BC/AD boundary (lower log, **Figure 2**). In these regards, it is difficult not to consider that these young ages determined from the bulk BS-1 and BS-3 samples are contaminated by modern roots and not representative of the age of the layer, and that the older ages of adjacent detrital charcoal samples record a closer approximation to the age of unit 2. Such an interpretation provides a logical explanation for bi-modal distribution of ages. To my knowledge, nowhere else in trenches along the Himalaya are sequences of radiocarbon ages are there any suggestions that detrital charcoal residence times approach 2000 years (see summary of **Wesnousky (2020)**). To end, the ages of samples taken from the Priyanka et al.'s unit 2 are ambiguous in asserting unit 2 was the ground surface in 1950 and, thus, whether or not earthquake displacement occurred in 1950.

The interpretation that unit 2 was the active soil in 1950 requires Units 3, 4, and 5 to have been deposited after the 1950 earthquake. The young and modern ages of samples P7 and P9 (upper and lower logs of **Figure 3**, respectively) are the primary evidence cited that the deposits hosting the samples were deposited after 1950. Theirlocations and context are shown in **Figure 4**. There are a number of reasons that draw the interpretation to be questioned. Numerous fine rootlets and burrow casts exist in the vicinity of the sample sites. There is the possibility that Priyanka et al. (2017) sampled decayed roots: no description of the samples (e.g., discrete or root-like) is provided in their work. More serious concern relates to the location and context of the samples. Priyanka et al. (2017) map the samples below a contact separating fine sands above (unit 5) from cleaner coarser sands below (unit 3) (**Figure SI3-1**). The change in color and texture at this level appears to mark the depth of active soil development and more aptly described as a soil horizon, not necessarily a contact between sediments deposited at different times. The darker redder tone (oxidation) and siltier component of unit 5 is the result of soil development on the sands of underlying unit 3. Although the authors indicate on their logs that the samples P7 and P9 were taken from the clean sands (unit 3), the photos of sample sites in **Figure 4** show they are near the base and within the zone of soil development (unit 5). It is common practice to avoid taking charcoal samples from within an active soil horizon because with ongoing soil processes the resulting ages will generally provide ages younger than the unit on which they are developed. Note that the sample P1 taken from the clean sand of unit 3 does give a much older age (Priyanka et al (2017) and also incorrectly place sample P1 in unit 2). Finally, if one allows that the P7 and P9 ages indicate a post-1950 age of unit 3, it is necessary that the oxidation and soil development embodied in unit 5 took place since 1950, a period of time of only 60-70 years or less. That is to say, in this authors view and experience, the amount of soil development in unit 5 is significantly more than expected in a 60-70 year period of time or less, and more similar to those observed at numerous trench sites along the arc where surfaces are known to be greater than 500 to 800 years. Additional supporting evidence for this latter conclusion is provided in the ensuing discussion. These observations diverge with interpretation that displacement of faults F1 and F2 occurred in 1950.

Unit 4 in Priyanka et al.'s (2017) trench log is presented as fault colluvium and Unit 5 as finer grain sediment deposited simultaneously. Three radiocarbon ages (P18, P6, and P3) are reported from these layers. P18 and P3 give ages close to the BC/AD boundary while P6 provides a modern post-1950 age. The sample P6 is thus critical to their interpretation of post 1950 rupture. The context of the P6 sample site is ambiguous and poor as it relates to argument that it provides clear evidence of a 1950 rupture. One may question why it was sampled. It appears it was sampled from a root scar associated with the now active soil and not a deposit that was present at the time of 1950 earthquake or emplaced shortly thereafter (**Figure 5**). It is a tenuous observation on which to firmly claim displacement occurred in 1950.

The Priyanka et al. (2017) trench is located near the northeastern end of the HFT fault scarp prior to disappearing into the Brahmaputra flood plain as it strikes northeastward (**Figure 6**). The trace of the fault scarp ends at approximately the road dividing the urbanized area from the vegetated area along the river. The vegetated area is the modern flood plain of the Brahmaputra and flow of the Brahmaputra has here removed the scarp. The exposure provided by excavation of a pit (Pit1) on the floodplain surface is shown in **Figure 7**, about 70 cm of clean white sand is seen overlying and in sharp contact with fine grained, oxidized, flood deposits which in turn rest on rounded fluvial gravel. The Pit 1 was excavated in 2014 AD. Fourteen years prior in 2000 AD there was a flood larger than any since before 1950 (Dasgupta and Mukhopadhyay, 2014). The river at that time rose 4.5 meters at Pasighat and the trench site is ~8-10 meters above that. The 14-year old capping clean white sands are virtually devoid of any sign of oxidation or soil development and are the ‘overbank’ deposit left by the flood. The sediments in the Pasighat trench (**Figure 7 lower**) are interpreted by the authors to post-date the 1950 earthquake. If correct, the sand of units 3 and 5 would be no more than ~ 64 years old at time of the excavation (2014-1950). For the authors interpretation that units 3 and 5 post date 1950, the flood sands deposited in the pit should 50 years from now reach a level of oxidation and soil development as observed in their trench walls. Given that virtually no oxidation or soil development has occurred since 2000 AD, this seems quite unlikely, and taken here as evidence that the deposits interpreted by the authors to post-date 1950 actually predate 1950 by a significant amount.

The subsequent study of Coudurier-Curveur et al (2020) of the 1950 earthquake reports to “provide new field evidence for its hitherto unknown surface rupture extent along the Mishmi and Abor Hills” that “attest to a minimum 200-km-long 1950 surface rupture on both the Mishmi and Main Himalayan Frontal Thrusts…” The following **Figure 08** taken from their paper shows the “Surface traces of the great, 15/8/1950, Assam earthquake….are outlined in red (dashed where inferred)” .

A major piece of evidence presented in support of their assertion that they observe scarps produced by the 1950 Assam earthquake is at Pasighat: *“Recently, however, in Pasigaht, ~400 m northeast of one roadside site previously identified to bear clear trace of the 1950 surface deformation (Figs. 2 and 6b; Kali et al., 2013; Coudurier-Curveur et al, 2014a, 2014b), shallow (~2 m) trenching has locally confirmed the existence of near surface faulting in the mid-20th century, hence likely in 1950 (Priyanka et al., 2017)”*. The citations of Kali and Coudurier-Curveur are unreviewed abstracts or conference presentations and by themselves are uninformative and provide no supporting evidence that may be reviewed in context of the interpretation that the scarp at Pasighat is due to 1950 displacement. The final phrase of the quoted statement cites Priyanka et al. (2017) as evidence supporting or guiding their conclusion that they observe 1950 surface rupture at Pasighat. The preceding discussion of that paper shows that observations presented by Priyanka et al. (2017) in support of the 1950 rupture are equivocal.

Figure 6 of the Coudrier-Curveur paper is reproduced in **Figure 9**. The figure caption indicates the figure shows the "1950 surface break along the Main Himalayan Thrust (MFT) at Pasighat". In the figure are three terraces (mapped as orange, yellow, green areas) that they interpret to be the result of 3 separate earthquake displacements, with the youngest being the green. Additionally they provide topographic profiles across each surface to illustrate the progressive offset of the surfaces. The location of the Priyanka et al. (2017) trench site is shown by an orange bar and letter T (**Figure 9**). It is puzzling and no discussion is provided concerning why the youngest green surface does not extend to the Priyanka et al. (2017) trench which they site in support of 1950 rupture. The Priyanka et al. (2017) trench is emplaced across a distinct scarp that is continuous from their trench southward to the surface mapped in green and the site shown in the photo labeled 'Pasighat Scarp 1'. Likewise the scarp height of 3.1 m at the Priyanka et al. (2017) trench site (**Figure 10**) is virtually identical to the Pasighat Scarp 1' scarp shown in **Figure 9**. Coudrier Curveur et al. (2020) conclude that the T1 surface is due to the 1950 earthquake though are no data presented to directly support the assertion. And again, the Priyanka et al. (2017) study provides at best equivocal support for their interpretation. Also shown are the ages of four ^{10}Be cosmogenic surface exposure ages for boulders on the T2 surface, all of which are greater than 2700 years. Granted the displacements responsible for the T1 and T2 surfaces likely post date this age, they are not evidence that displacement occurred in 1950. It might be speculated that the most recent is from 1950 but direct evidence is absent.

Figure 5 of Coudurier-Curveur (2020) shows a similar instance of two progressively offset terraces, profiles across the terraces, cosmogenic surface exposure ages of boulders on the surfaces, and is reproduced in **Figure 11**. Again the caption and text indicate clearly the authors' interpretation that the trace moved in 1950 and it is concluded that the terrace (colored yellow) across which Profile 1 is measured is the result of 7.6 m of vertical displacement in 1950. Evidence they cite in support of their conclusion is a ^{10}Be cosmogenic surface exposure age of one of two boulders sampled from the T1 (yellow) surface and the shape of the scarp. The surface exposure ages for two boulders sampled from the P1 are reportedly ~173 years and the other ~1188 years. The authors choose the 173 year as representative and discard the 1188 year age. With two ages, and in an environment of such rainfall and vigorous erosion, it is equally plausible that the younger age simply reflects a recent denudation or disturbance of the ground around the sample site or that root movement has more recently exposed the boulder in this heavily forested area (**Figure 11**).

The authors further state "Considering the steep, fresh morphology of the Kamlang scarp, we interpret the youngest cosmogenic age to constrain the onset of floodplain abandonment and therefore the maximum age of co-sesmic offset uplift. In all likelihood, such very recent abandonment should be correlated with the 1950 Assam earthquake, the only known regional event in the entire region large enough to produce the particularly high uplift along the Kamlang terrace". A reader should consider the context of the reasoning. Any systematic accounting of earthquakes in the regions extends back only to the middle of the 19th century (Poddar, M. C. , 1952, Bulletins of the Geological Survey of India. Series B, Engineering geology and groundwater. Preliminary report of the Assame earthquake, 15th August 1950). The authors provide no citation to view the context of the statement. As such, the historical record cannot be used to rule out the scarp significantly predates 1950. The observation of 'the steep, fresh morphology' of the scarp shown in **Figure 11** may also be questioned as basis to conclude the scarp across the P1 surface is 1950. The authors site the form and steepness of the Kamlang scarp shown in **Figure 11** to be similar to those formed during the recent 1999 Mw 7.6 Chi-Chi earthquake and reason to assert the 1950 genesis of the Kamlang scarp. But it is not **(Figure 12**). The Chi-Chi scarp is the result of folding and the steep scarp face is a dip panel. In contrast, there is no folding preserved in the capping deposits at the 7.6 m Wakro scarp in **Figure 11.** The observed scarp is erosional. With respect to the freshness and steepness of the scarps at Kamlang and described elsewhere in this paper, they are qualitatively no 'fresher' or steeper than scarps observed at trench sites along the HFT. Scarps at Tribeni and Bagmati in Nepal are clear examples which, after being produced ~1000 years ago, still preserve dip panels (Wesnousky et al., 2017a). That is to say, there is no basis to assess the age of Himalayan thrust faults on the basis of fault scarp steepness. In sum, the comparison of scarp slopes and forms observed at Kamlang to those formed in Chi-Chi as a basis to assert age of Kamlang scarp formation is not a strong foundation on which to rest interpretation of 1950 surface rupture.

The site of Marbang is annotated on **Figure 8**. The location is that of a trench study along the Himalayan frontal thrust (Jayangondaperumal et al., 2011). Coudurier-Curveur et al. (2020) largely ignore the study though it is of significant consequence to their conclusion of 1950 surface rupture. The well-defined 8 m scarp at Marbang is only ~12 km southwest of Pasighat and on the same fault trace the authors interpret to record 1950 rupture (**Figure 8**). The Marbang trench log is reproduced in **Figure 13**.

Structural and stratigraphic relationships exposed in the Marbang trench preclude that the scarp was involved in a 1950 rupture. The growth stratigraphy of unit 4 is horizontal and in angular unconformity with the underlying unit 3 growth package. The underlying unit 3 package was tilted by an earthquake that preceded the deposition of unit 4: unit 4 was deposited shortly after tilting of unit 3 and unit 4 was deposited subsequent to an earlier earthquake. Radiocarbon samples extracted from unit 4 are on the range of 2000 years old. If an earthquake as large as interpreted by the authors occurred in 1950, the unit 4 sediments would be deformed. They are not. Rather, the untilted 2000 year old sediments are evidence against surface rupture having occurred during 1950. This is quite in contrast to the Coudurier-Curveur et al (2020) characterization of the paper: "..despite dedicated research (e.g. …Jayangondaperumal et al, 2011), no unequivocal evidence of a primary surface rupture was found for a long time". The Priyanka et al. (2017) paper also ignores this site.

The 1950 fault trace interpreted and mapped by Coudurier-Curveur et al (2020) continues southward from Marbang across a step in fault trace a distance of about 8 km to Niglok (**Figure 14**). Evidence that scarps at Niglok record 1950 surface rupture is limited in Coudurier-Curveur et al. (2020) to photos of the scarp (their Figures 4a and S2) and comment on its fresh appearance. The author has observed and reported on numerous scarps along the HFT that date back more than 500 years (e.g., Wesnousky, 2020) and give 'fresh appearance', so the photo is not robust evidence of 1950 rupture. Priyanka (2019) , from study of exposure provided by two trenches emplaced across the Niglok scarps (**Figure 14**), independently interprets displacement on the Niglok scarps occurred in both the Sadiya earthquake of 1697 and the great Assam earthquake of 1950. I was provided the opportunity to visit and independently log the excavations. The logs I constructed of the two trenches are combined with the radiocarbon ages published by Priyanka (2019) and provided in **Figures 15** and **16**. The main similarities of the two trench sites are that (1) they are across scarps asserted to record surface rupture in 1950, (2) each is across a morphologically well preserved scarp, (3) the fault responsible for creation of the scarp is clear and extends to near the surface in each exposure, and (4) there is no evidence to clearly supporting the authors assertion that rupture occurred here in 1950. The latter point warrants explanation: Initially consider that the deposits colored yellow on the footwall of each surface are growth stratigraphy deposited subsequent to the last fault displacement.

Detrital charcoal in the deposits is invariably many hundreds of years old, allowing that they were deposited significantly prior to the most recent displacement in 1950. One may alternately consider that the footwall deposits existed and were faulted at time of last displacement and arrive at a similar result: the most recent displacement occurred after a time many centuries ago. Neither interpretation yields clear and direct evidence of 1950 rupture.

Log of Trench 01 in **Figure 15** shows fine grained growth stratigraphy (yellow units 1 to 4) resting on faulted fluvial gravel and truncation of Siwalik bedrock on the hanging wall. The ages of detrital charcoal are also plotted in **Figure 15** according to stratigraphic horizon they are sampled. The detrital charcoal ages from unit 1 range from 83 BC to 1475 AD. To interpret that the unit 1 deposit actually post-dates 1950 requires an assumption that the residence time of detrital charcoals prior to being deposited here is at minimum 500 years and up to 2000 years. Alternately allowing that unit 1 existed at the time of last fault displacement at best places the displacement at post 1475AD, well before 1950, unless again an assumption of long residence times is assumed for the samples. Either way, any interpretation favoring 1950 surface rupture here will necessarily be based on assumption and an alternate interpretation that the most recent surface rupture predates 1950 equally valid.

Unit 7 of the trench 02 log shown in **Figure 16** is fine-grained sediment analogous to modern overbank flood deposits. The unit appears to be faulted. Ages in the unit cluster around the AD/BC boundary. Accepting the interpretation, it may only be said that displacement occurred around or after the AD/BC boundary. If one is to assert that displacement occurred in 1950, it requires detrital charcoal resident times of a couple of thousand years. Radiocarbon ages for samples taken from Unit 7w are stratigraphically and radiometrically younger than those taken from underlying unit 7. The ages are bracketed between 1477 to 1654 AD. If deposited after the most recent offset, they suggest the event occurred well prior to 1950 , unless it is assumed that each is characterized by residence times of hundreds of years. In any case, any interpretation of 1950 displacement here would be based on assumption and not definitive evidence.

Alternately, if deposits of unit 7w are considered to have been deposited prior to the most recent displacement, they only provide information that displacement occurred after 1477 to 1654 AD and one must again assume long residence times to arrive at the conclusion that 1950 displacement is recorded in the exposure. While one may consider the assumptions to yield a 1950 interpretation reasonable, they do not lead to proof of 1950 displacement. Indeed, observations can equally if not more likely be interpreted to reflect pre-1950 displacement.

The sum of observations does not preclude the possibility that surface rupture occurred in 1950. They do though in my view show that neither of the two papers provide substantive, definitive, quantitative evidence that the 1950 Assam earthquake produced surface rupture along the HFT. The interpretations of 1950 surface rupture at any particular site much less along a continuous 200 km section of the Himalayan front are based on assumption and circumstantial evidence and there are observations that contradict their conclusions. An unfortunate consequence of the papers is that the findings taken at face value and not considered carefully may serve to stymie future investigators from further efforts to find whether or not surface rupture along the HFT or elsewhere accompanied the 1950 Assam earthquake. At this time, clear and substantive evidence does not exist.

Discussion and Conclusion.

The ~Mw 8.7-8.9 June 6 1505 (central Himalaya), the Mw 8.4 Jan 15, 1934 (Bihar), and the Mw 8.7 Aug 15, 1950 (Assam) earthquakes are the largest documented in the historical record. A considered view of the observations reveals no clear and substantive evidence that any of them produced surface rupture along the Himalayan Frontal Thrust. The logical implication then is that the paleoearthquake magnitude detection level for earthquakes on the MHT is on the order of Mw >8.7. One may entertain the suggestion that scarps formed during these three particular large earthquakes have been eroded or buried, but it is difficult to reconcile with the existence of numerous much older uneroded large fault scarps in young alluvium at places along the entire length of the HFT (Wesnousky, 2020). On a practical level then, the observations remain pointing to a paleoearthquake detection level threshold of Mw > 8.7. The result does not preclude lesser sized earthquakes from producing surface rupture along the HFT at some time but, with the observations in hand, paleoseismology cannot be expected to consistently provide a complete geologically recorded history of events at or below ~Mw 8.7. Further search for evidence of surface rupture attendant to these largest of Himalayan earthquakes along the HFT remains warranted and encouraged.

Acknowledgements

I thank Dr. Jayangandoperumal for the invitation to independently view and study the trenches excavated during his project. Center for Neotectonic Studies Contribution #.

References

Ambraseys, N., Jackson, D., 2003. A note on early earthquakes in northern India and southern Tibet. Current Science 84, 570-582.

Angster, S., Fielding, E.J., Wesnousky, S., Pierce, I., Chamlagain, D., Gautam, D., Upreti, B.N., Kumahara, Y., Nakata, T., 2015. Field reconnaissance after the 25 April 2015 M 7.8 Gorkha earthquake. Seismological Research Letters 86, 1506-1513.

Berthet, T., Ritz, J.-F., Ferry, M., Pelgay, P., Cattin, R., Drukpa, D., Braucher, R., Hetenyi, G., 2014. Active tectonics of the eastern Himalaya: New constraints from the first tectonic geomorphology study in southern Bhutan. Geology 42, 427-430.

Bilham, R., 2018. Himalayan Earthquakes: A Modern Synthesis. Geophysical Society of London Special Publication 18-122, in review.

Bollinger, L., Sapkota, S.N., Tapponnier, P., Klinger, Y., Rizza, M., Van der Woerd, J., Tiwari, D.R., Pandey, R., Bitri, A., de Berc, S.B., 2014. Estimating the return times of great Himalayan earthquakes in eastern Nepal: Evidence from the Patu and Bardibas strands of the Main Frontal Thrust. Journal of Geophysical Research-Solid Earth 119, 7123-7163.

Coudurier-Curveur, A., Tapponnier, P., Okal, E., Van der Woerd, J., Kali, E., Choudhury, S., Baruah, S., Etchebes, M., Karakas, C., 2020. A composite rupture model for the great 1950 Assam earthquake across the cusp of the East Himalayan Syntaxis. Earth and Planetary Science Letters 531, 12 pp.

Dasgupta, S., Mukhopadhyay, B., 2014. Earthquake – Landslide - Flood nexus at the lower reaches of Yigong Tsangpo, Tibet: Remote control for catastrophic flood in Siang, Arunachal Pradesh and Upper Assam, India. Journal of Engineering Geology [A bi-annual journal of ISEG] 39, 177-190.

Hayes, G.P., Briggs, R.W., Barnhart, W.D., Yeck, W.L., McNamara, D.E., Wald, D.J., Nealy, J.L., Benz, H.M., Gold, R.D., Jaiswal, K.S., Marano, K., Earle, P.S., Hearne, M.G., Smoczyk, G.M., Wald, L.A., Samsonov, S.V., 2015. Rapid Characterization of the 2015 M-w 7.8 Gorkha, Nepal, Earthquake Sequence and Its Seismotectonic Context. Seismological Research Letters 86, 1557-1567.

Hetenyi, G., Le Roux-Mallouf, R., Berthet, T., Catting, R., Cauzzi, C., Phuntsho, K., Grlimund, R., 2016. Joint approach combining damage and paleoseismology observations constrains the 1714 A. D. Bhutan earthquake at magnitude 8 ± 0.5. Geophys. Res. Lett. 43, 10,695-610,702.

Jackson, D., 2002. The great western-Himalayan earthquake of 1505: A rupture of the central Himalayan Gap?, Tibet, past and present: Tibetan studies 1; Proceedings of the ninth seminar of the International Association for Tibetan Studies, Leiden, Netherlands, pp. 147-158.

Jayangondaperumal, R., Wesnousky, S.G., Choudhuri, B.K., 2011. Near-Surface Expression of Early to Late Holocene Displacement along the Northeastern Himalayan Frontal Thrust at Marbang Korong Creek, Arunachal Pradesh, India. Bulletin of the Seismological Society of America 101, 3060-3064.

Kumar, S., Wesnousky, S.G., Rockwell, T.K., Briggs, R.W., Thakur, V.C., Jayangondaperumal, R., 2006. Paleoseismic evidence of great surface rupture earthquakes along the Indian Himalaya. Journal of Geophysical Research-Solid Earth 111.

McCalpin, J., 1996. Paleoseismology, 1st edition ed. Academic Press, New York.

McCalpin, J., 2009. Paleoseismology, 2nd edition ed. Academic Press, New York.

Pant, M.R., 2002. A step towards a historical seismicity of Nepal, ADARSA. Pundit publications, Kathmandu, pp. 29-60.

Priyanka, R.S., 2019. Surface rupture investigations of the meisoseismal zone of Assam earthquake along Himalayan Foothill Zone Arunachal Pradesh Assam Himalaya, Geology. Kumaun University, India, http://hdl.handle.net/10603/313858, p. 356 p.

Priyanka, R.S., Jayangondaperumal, R., Pandey, A., Mishra, R.L., Singh, I., Bhushan, R., Srivastava, P., Ramachandran, S., Shah, C., Kedia, S., Sharma, A.K., Bhat, G.R., 2017. Primary surface rupture of the 1950 Tibet-Assam great earthquake along the eastern Himalayan front, India. Sci Rep 7, 12.

Sapkota, S.N., Bollinger, L., Klinger, Y., Tapponnier, P., Gaudemer, Y., Tiwari, D., 2013. Primary surface ruptures of the great Himalayan earthquakes in 1934 and 1255. Nature Geoscience 6, 71-76.

USGS, 2021. A list of the 20 largest earthquakes in the world. website accessed May 1, 2021: https://www.usgs.gov/natural-hazards/earthquake-hazards/science/20-largest-earthquakes-world?qt-science_center_objects=0#qt-science_center_objects.

Wesnousky, S.G., 1986. Earthquakes, Quaternary faults, and seismic hazard in California. Journal of Geophysical Research-Solid Earth and Planets 91, 2587-2631.

Wesnousky, S.G., 2008. Displacement and geometrical characteristics of earthquake surface ruptures: Issues and implications for seismic-hazard analysis and the process of earthquake rupture. Bulletin of the Seismological Society of America 98, 1609-1632.

Wesnousky, S.G., 2020. Great pending Himalayan earthquakes. Seismological Research Letters 91, 3334-3342.

Wesnousky, S.G., Kumahara, Y., Chamlagain, D., Pierce, I.K., Karki, A., Gautam, D., 2017a. Geological observations on large earthquakes along the Himalayan frontal fault near Kathmandu, Nepal. Earth and Planetary Science Letters 457, 366-375.

Wesnousky, S.G., Kumahara, Y., Nakata, T., Chamlagain, D., Neupane, P., 2018a. New Observations Disagree With Previous Interpretations of Surface Rupture Along the Himalayan Frontal Thrust During the Great 1934 Bihar-Nepal Earthquake. Geophysical Research Letters 45, 2652-2658.

Wesnousky, S.G., Scholz, C.H., Shimazaki, K., Matsuda, T., 1984. Integration of geological and seismological data for the analysis of seismic hazard - a case-study of Japan. Bulletin of the Seismological Society of America 74, 687-708.

Figure Captions.

Figure 1. (Bottom left inset) General plate tectonic framework showing convergence of India into Tibet along arcuate zone of thrusting (The Himalayan arc). (top right inset) generalized north–south cross-section transverse to Himalayan arc shows location of Main Himalayan thrust (MHT) décollement and intersections with surface that define the HFT and MBT and location of contemporary moderate size earthquakes. Location of paleoearthquake studies shown by solid dots. Synopsis and citations to original studies are in Wesnousky (2020). Blue and green dots cited specifically in text are from Kumar et al. (2006) and Le Roux-Mallouf et al. (2016). Red dots are locations of felt reports used by Jackson (2002) to interpret 1505 earthquake is possibly result of slip on the Main Himalayan Thrust.Yellow stars are locations of felt reports reported by Hetenyi et al. (2016) to interpret source area of 1714 earthquake. Magnitudes and approximate source areas from Bilham (2018).

Figure 2. (a) Reproduction of both sides of Pasighat trench wall presented by Priyanka et al. (2017) showing location and ages of radiocarbon samples. (b) Radiocarbon ages from both trenches replotted with Oxcal (Ramsey, 1955) and grouped according to unit from which authors report they are sampled and arranged in stratigraphic order. Sample names at left of each plot end indicate unit from which sample taken. Plot on right is same as left except horizontal axis expanded to more clearly show ages. Vertical blue line marks 1950. Blue dots with arrows are samples reported to be radiocarbon ‘modern’ post 1950.

Figure 3. Images of Bulk Sample locations from unit 2. Modern roots are abundant in the unit 2 layer from which bulk samples yield modern ages, yet adjacent discrete detrital ages from same unit yield significantly older ages.

Figure 4. The young and modern ages of samples P7 and P9 are used as primary evidence that the deposits in which they were taken were deposited after 1950. See text for discussion.

Figure 5. Sample P6 located at orange flag in geologic context.

Figure 6. Location of Priyanka et al. (2017) trench in context of trace of HFT (red line) and Pit excavated on Brahmaputra flood plain.

Figure 7. Soil development on sands from 2000 Brahamaputra River flood is markedly less where exposed in a pit (upper) in comparison to that developed on the upper layers of the Priyanka et al. (2017) trench wall that are interpreted to post date 1950.

Figure 8. Reproduction of Coudurier-Curver et al. (2017) figure where within they describe“surface traces of the great, 15/8/1950, Assam earthquake rupture on Main Himalayan Frontal Thrust (MFT) and Mishmi Thrust (MT) are outlined in red (dashed where inferred along Manabhum anticline front” The locations of Marbang and Niglok are added here.

Figure 9. Reproduction of Coudurier-Curver, et al. (2017) Figure 6 that is described as “1950 surface break along the Main Himalayan Frontal Thrust”.

Figure 10. Profile and photo of scarp at Pryanka et al. (2017) trench site. The location of the trench site is marked by T in Figure 9 and the observed scarp may be followed continuously to the south and the surface delineated T1 in Figure 9.

Figure 11. Reproduction of Coudurier-Curveur (2020) figure 5 showing scarps and terraces at Kamlang.

Figure 12. Images of 1999 Chi-Chi earthquake scarp put forth by Coudurere-Curveur (2020) as analog and support for interpretation that scarp shown in Figure 11b is result of surface slip in 1950. The clear presence of folding and presence of a dip panel that is commonly preserved on scarps approaching 1000 years along the length of the HFT and for the 1999 Chi-Chi scarps is not evident at Wakro.

Figure 13. Reproduction of Jayangandoperumal et al.’s 2011 trench log at Marbang. See Figure 8 for regional Location.

Figure 14. Map of fault trace, progressively offset terraces, and trench sites near Niglok. Site location labeled on regional map of Figure 8.

Figure 15. Log and photo of Trench 01 at Niglok. Plot of radicarbon ages at right. Location on Figure 14.

Figure 16. Trench log and Photos of Niglok Trench 2.

Figures (and captions)

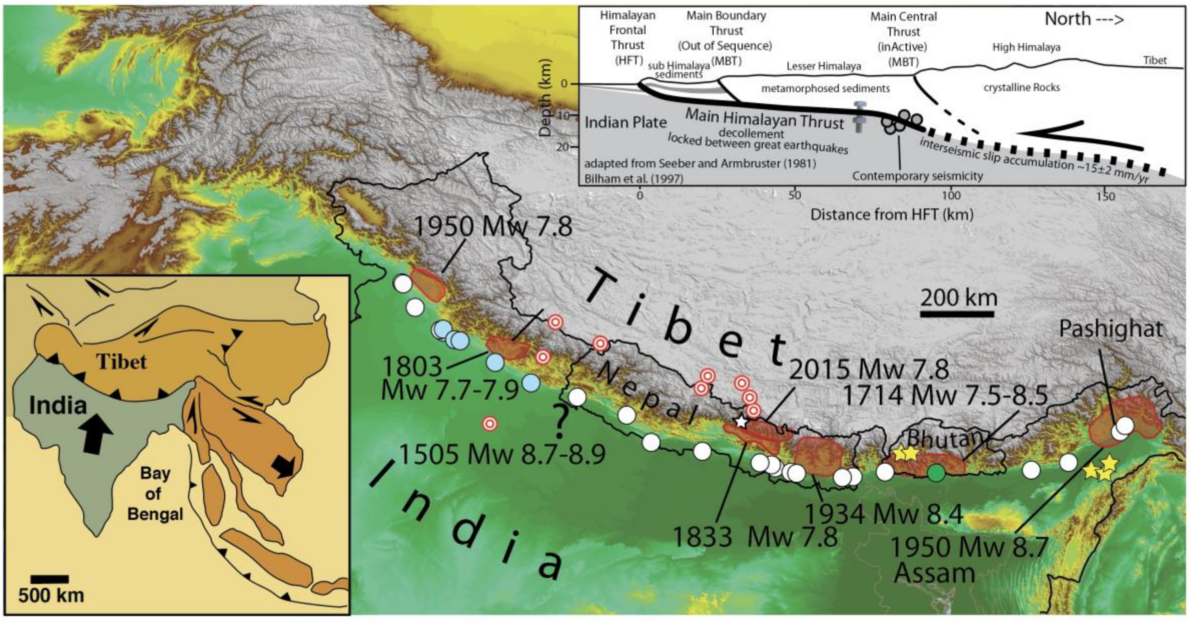

Figure 1. (Bottom left inset) General plate tectonic framework showing convergence of India into Tibet along arcuate zone of thrusting (The Himalayan arc). (top right inset) generalized north–south cross-section transverse to Himalayan arc shows location of Main Himalayan thrust (MHT) décollement and intersections with surface that define the HFT and MBT and location of contemporary moderate size earthquakes. Location of paleoearthquake studies shown by solid dots. Synopsis and citations to original studies are in Wesnousky (2020). Blue and green dots cited specifically in text are from Kumar et al. (2006) and Le Roux-Mallouf et al. (2016). Red dots are locations of felt reports used by Jackson (2002) to interpret 1505 earthquake is possibly result of slip on the Main Himalayan Thrust.Yellow stars are locations of felt reports reported by Hetenyi et al. (2016) to interpret source area of 1714 earthquake. Magnitudes and approximate source areas from Bilham (2018).

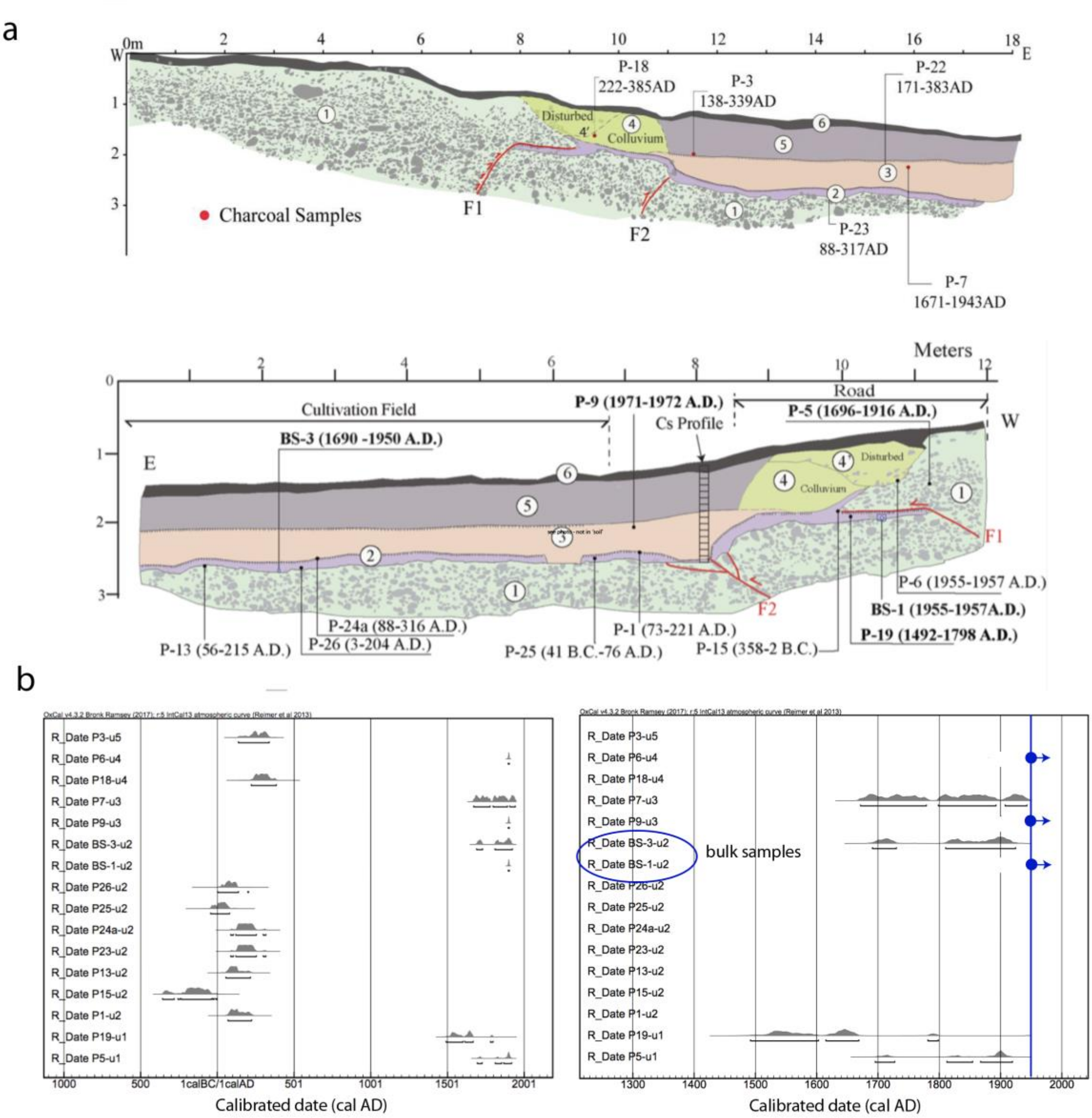

Figure 2. (a) Reproduction of both sides of Pasighat trench wall presented by Priyanka et al. (2017) showing location and ages of radiocarbon samples. (b) Radiocarbon ages from both trenches replotted with Oxcal (Ramsey, 1955) and grouped according to unit from which authors report they are sampled and arranged in stratigraphic order. Sample names at left of each plot end indicate unit from which sample taken. Plot on right is same as left except horizontal axis expanded to more clearly show ages. Vertical blue line marks 1950. Blue dots with arrows are samples reported to be radiocarbon 'modern' post 1950.

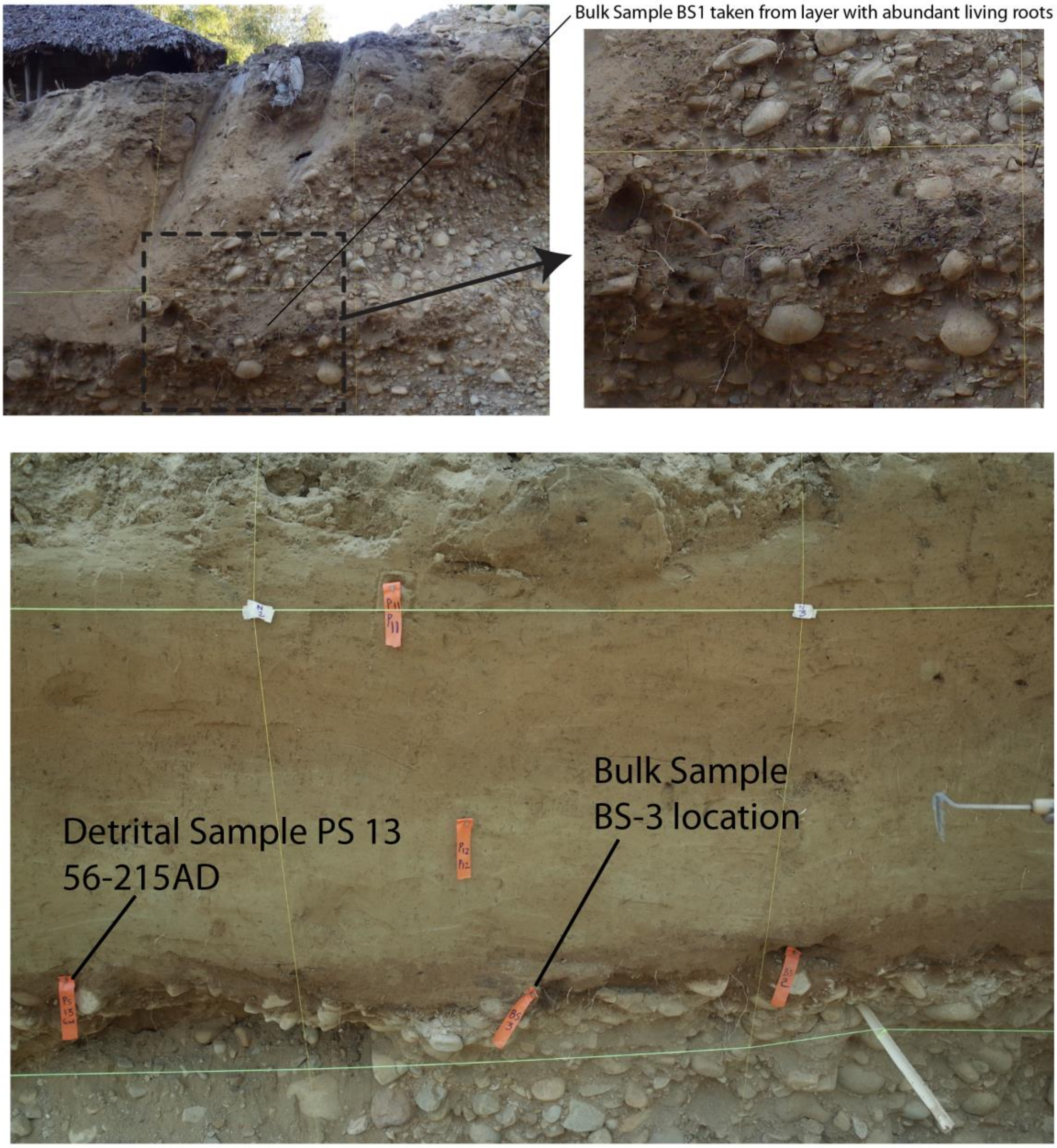

Figure 3. Images of Bulk Sample locations from unit 2. Modern roots are abundant in the unit 2 layer from which bulk samples yield modern ages, yet adjacent discrete detrital ages from same unit yield significantly older ages

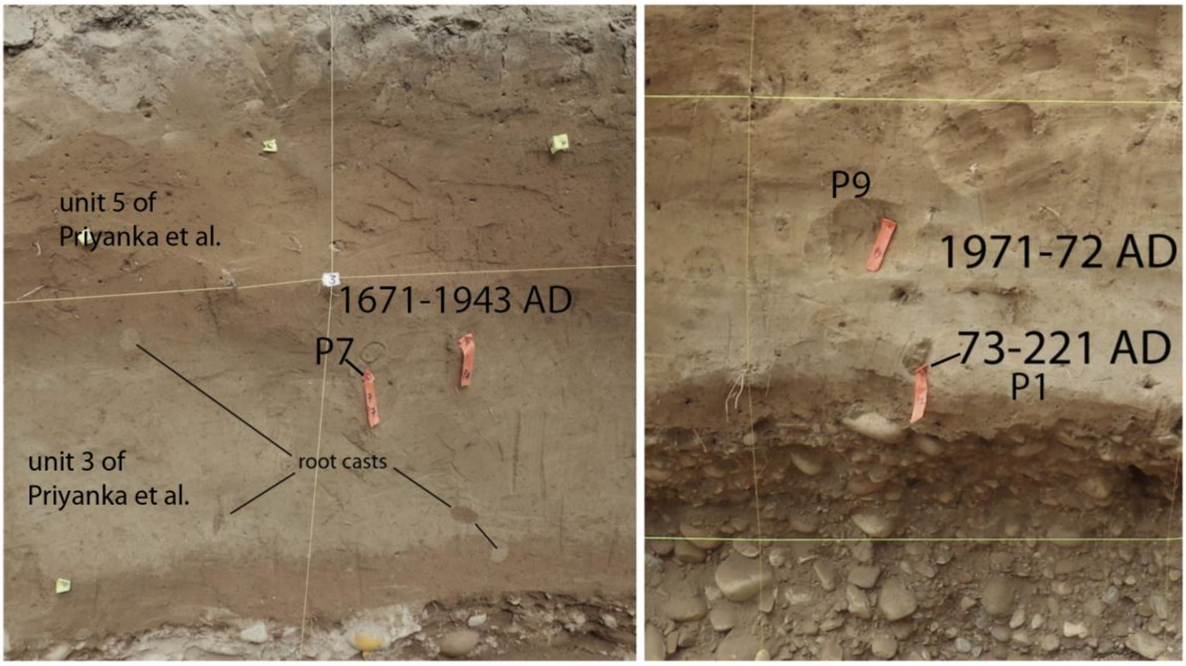

Figure 4. The young and modern ages of samples P7 and P9 are used as primary evidence that the deposits in which they were taken were deposited after 1950. See text for discussion.

Figure 5. Sample P6 located at orange flag in geologic context.

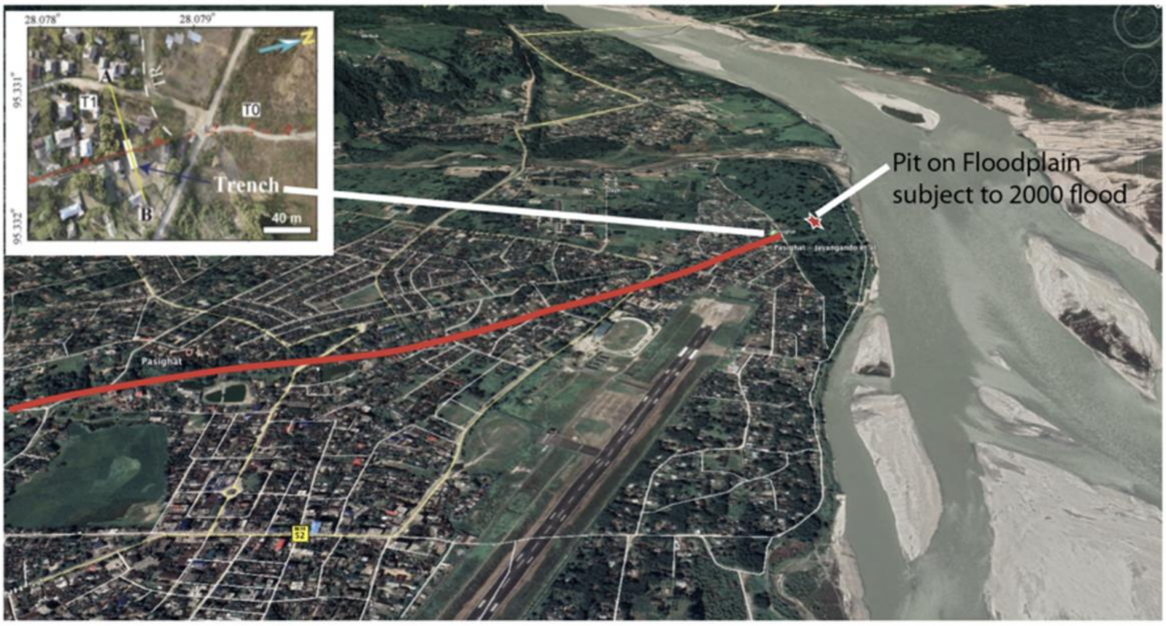

Figure 6. Location of Priyanka et al. (2017) trench in context of trace of HFT (red line) and Pit excavated on Brahmaputra flood plain.

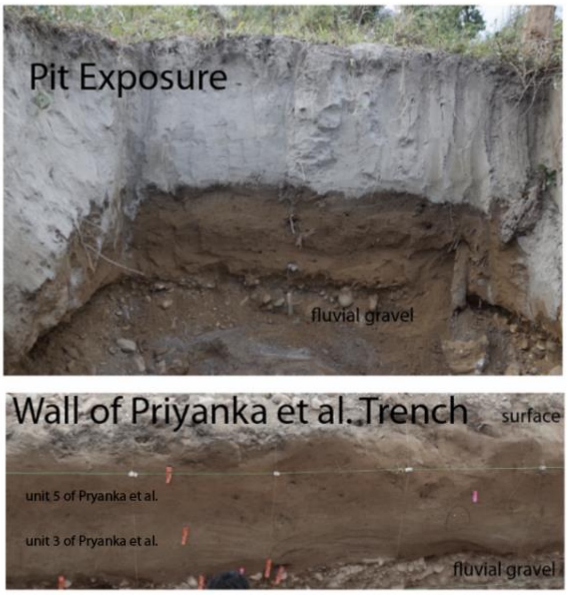

Figure 7. Soil development on sands from 2000 Brahamaputra River flood is markedly less where exposed in a pit (upper) in comparison to that developed on the upper layers of the Priyanka et al. (2017) trench wall that are interpreted to post date 1950.

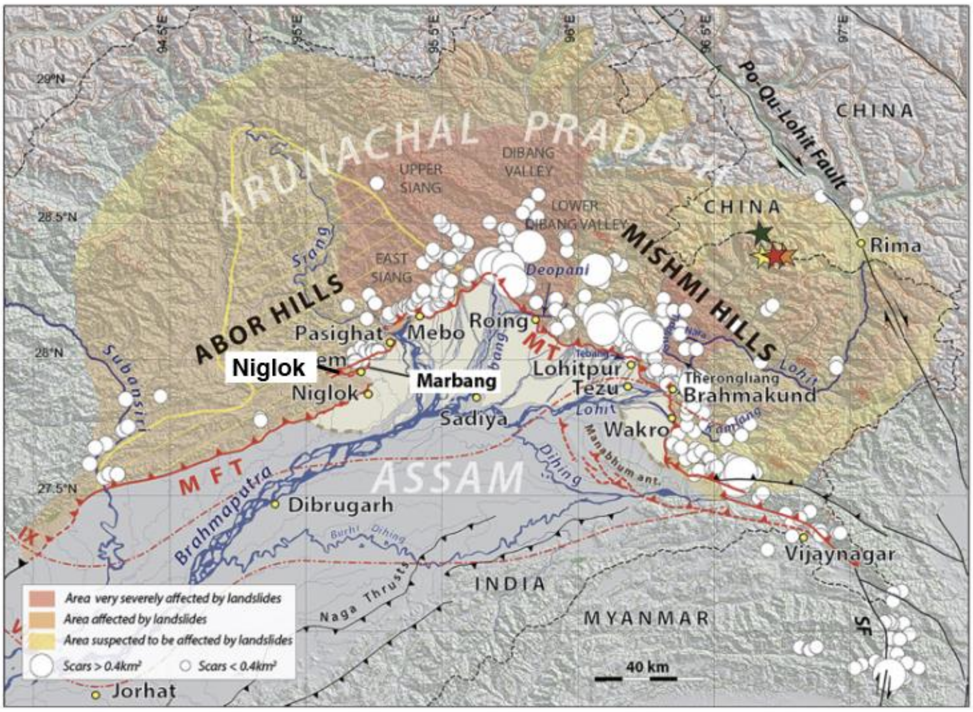

Figure 8. Reproduction of Coudurier-Curveur et al. (2017) figure where within they describe "surface traces of the great, 15/8/1950, Assam earthquake rupture on Main Himalayan Frontal Thrust (MFT) and Mishmi Thrust (MT) are outlined in red (dashed where inferred along Manabhum anticline front" The locations of Marbang and Niglok are added here.

Figure 9

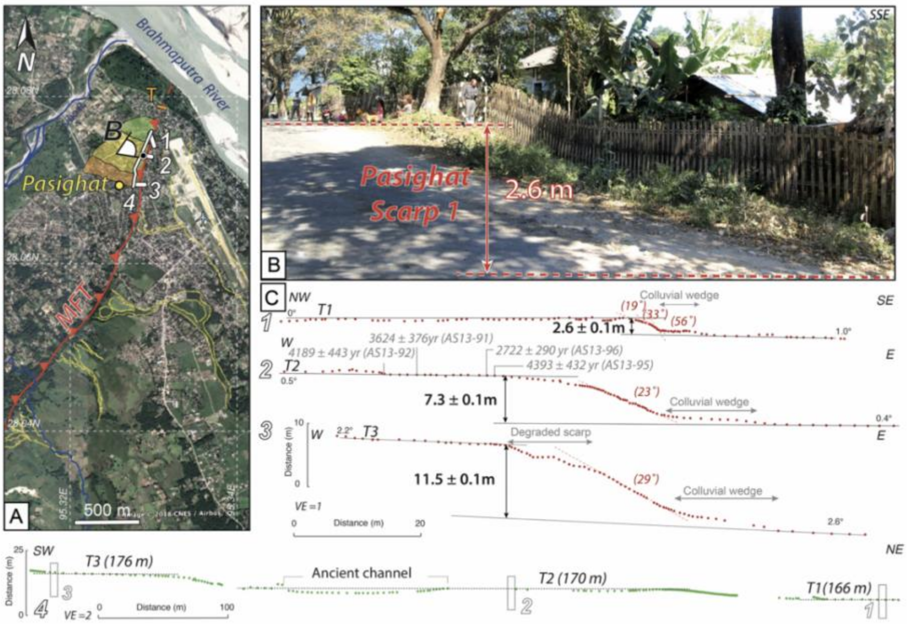

Figure 9. Reproduction of Coudurier-Curver, et al. (2017) Figure 6 that is described as "1950 surface break along the Main Himalayan Frontal Thrust".

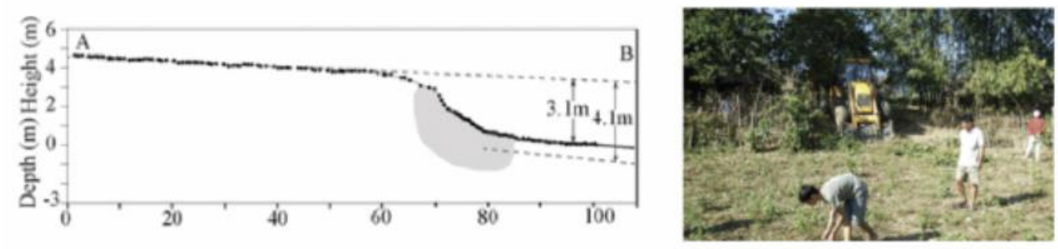

Figure 10. Profile and photo of scarp at Pryanka et al. (2017) trench site. The location of the trench site is marked by T in Figure 9 and the observed scarp may be followed continuously to the south and the surface delineated T1 in Figure 9.

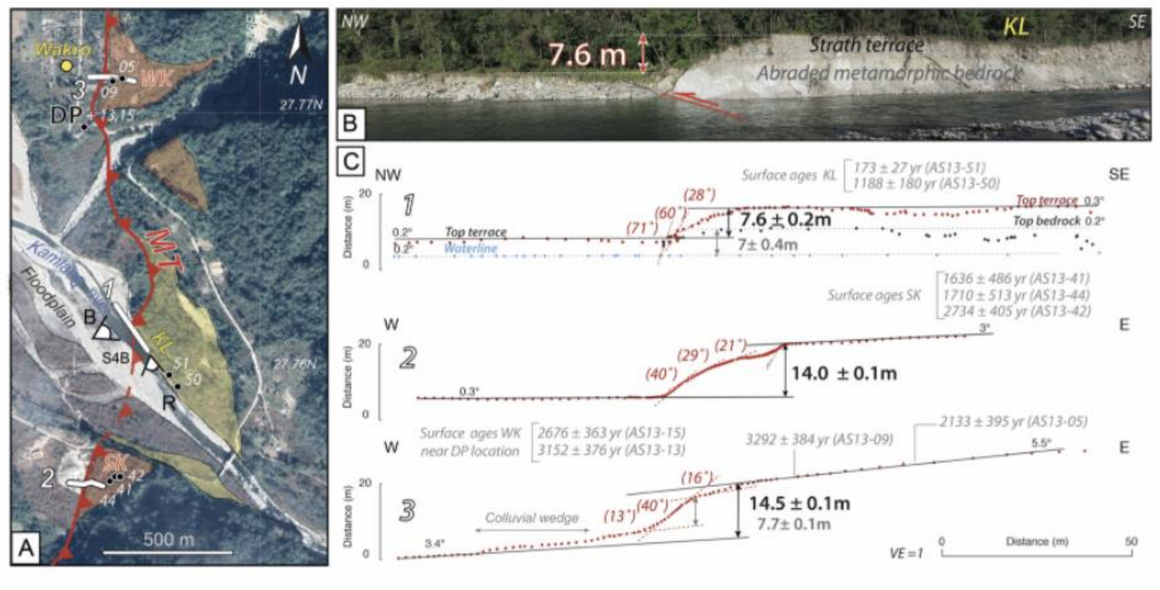

Figure 11. Reproduction of Coudurier-Curveur (2020) figure 5 showing terraces at Kamlang.

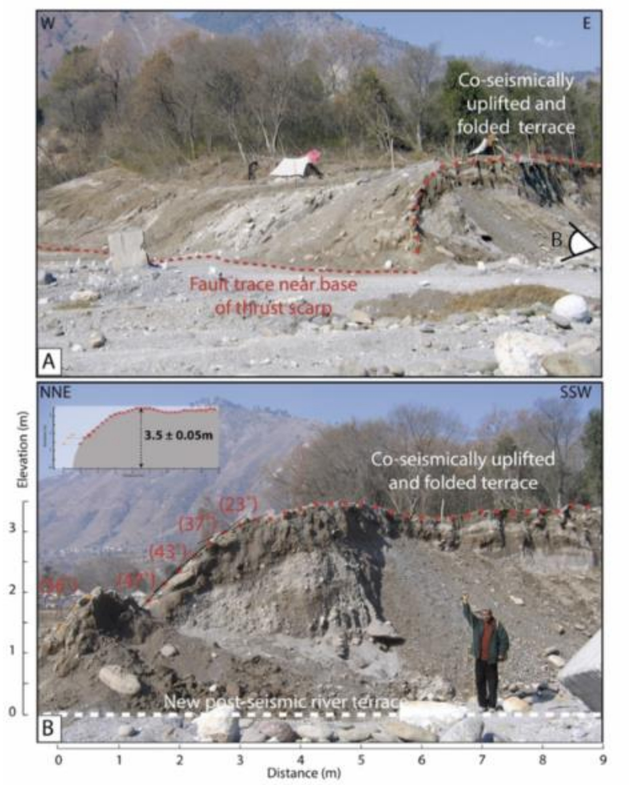

Figure 12. Images of 1999 Chi-Chi earthquake scarp put forth by Coudurere-Curveur (2020) as analog and support for interpretation that scarp shown in Figure 11b is result of surface slip in 1950. The clear presence of folding and presence of a dip panel that is commonly preserved on scarps approaching 1000 years along the length of the HFT and for the 1999 Chi-Chi scarps is not evident at Wakro.

13.

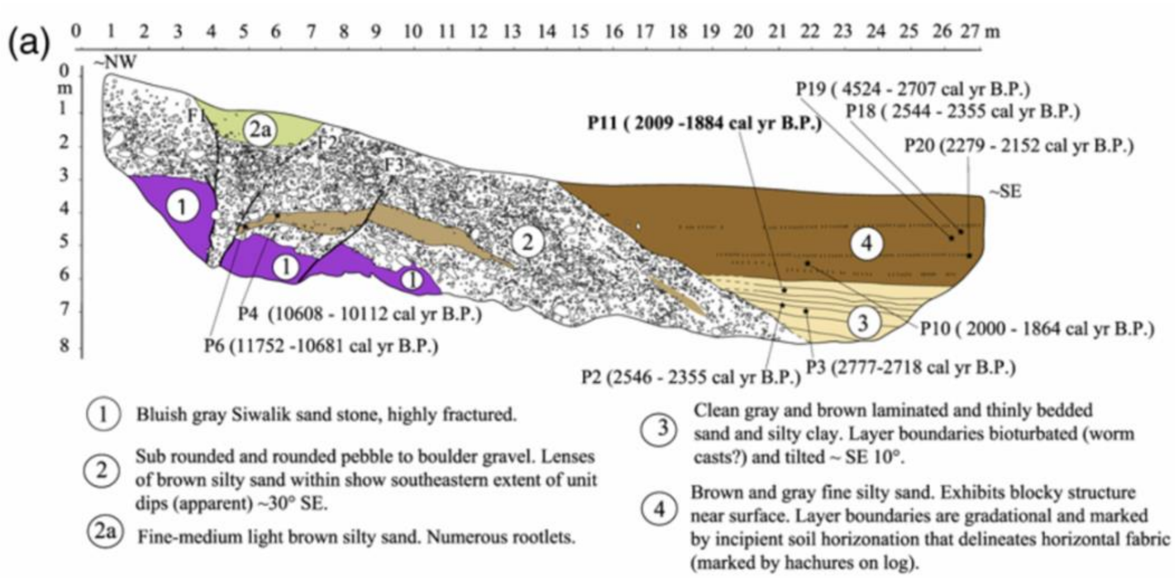

Figure 13. Reproduction of Jayangandoperumal et al.'s 2011 trench log at Marbang. See Figure 8 for regional location.

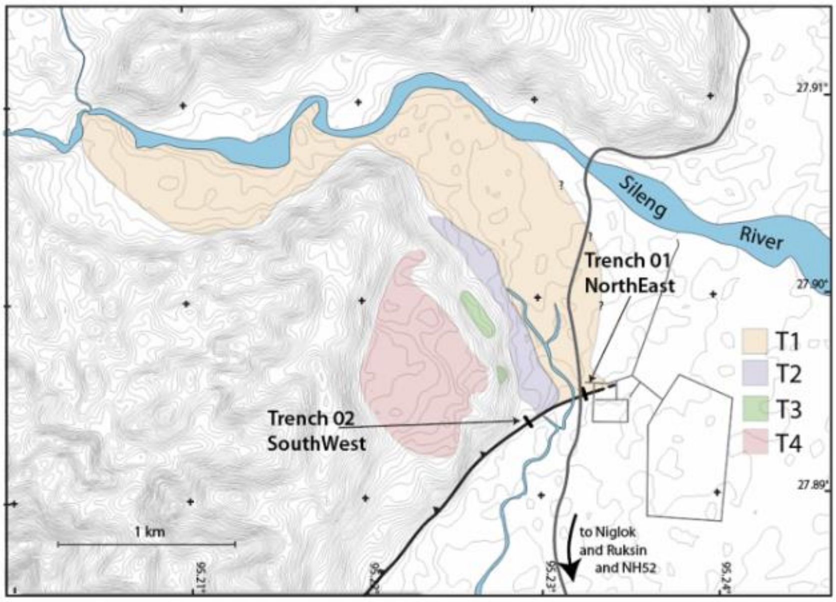

Figure 14. Map of fault trace, progressively offset terraces, and trench sites at Niglok. See Figure 8 for regional location.

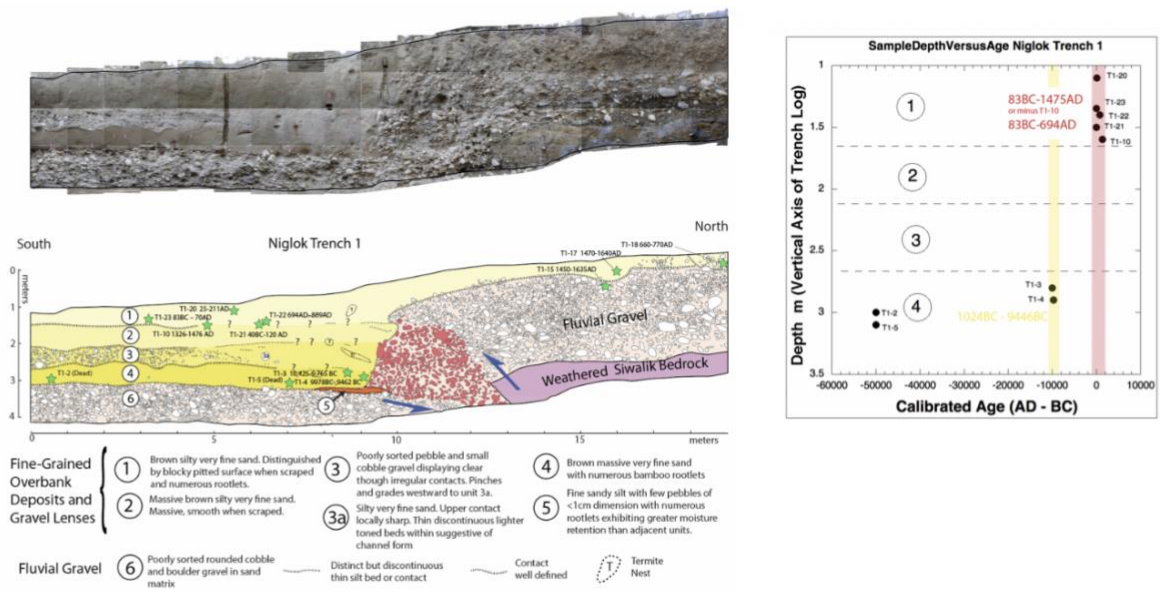

Figure 15. Log and photo of Trench 01 at Niglok. Plot of radicarbon ages at right. Location on Figure 14.

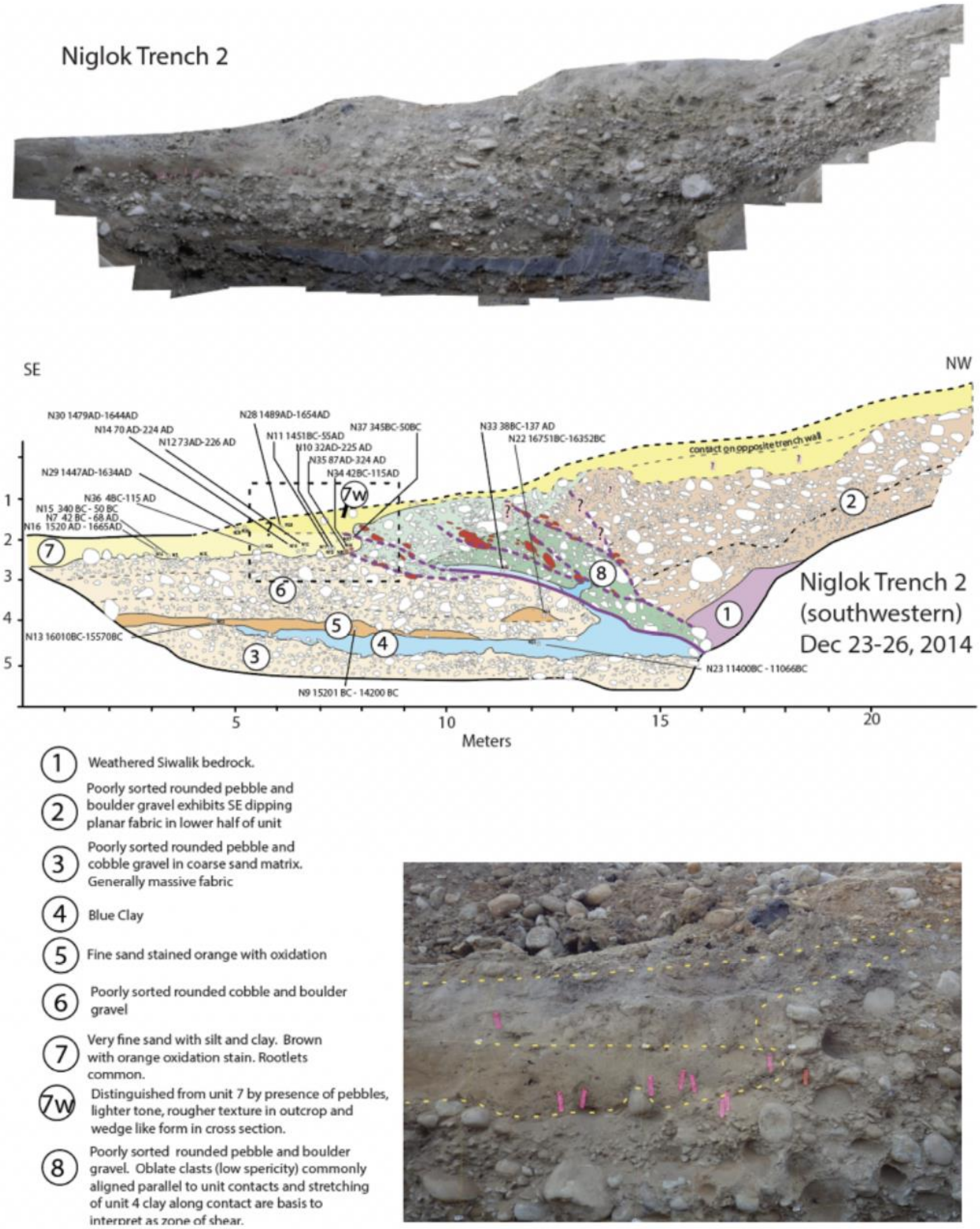

Figure 16. Trench log and Photos of Niglok Trench 2.